Supporting Information

Hot adsorbate-induced retardation of the internal thermalization of nonequilibrium electrons in adsorbate-covered metal nanoparticles

Christophe Bauer, Jean-Pierre Abid and Hubert H. Girault
Laboratoire d'Electrochimie Physique et Analytique
Faculté des Sciences de Base
Ecole Polytechnique Fédérale de Lausanne
CH-1015 Lausanne, Switzerland

Box 1.

Preparation and structure of the 3 dimensional samples.

Advantages of these samples to study interfacial phenomena by transient absorption spectrosopy.

We use "soft" surface science approach to prepare the samples, that permit the investigation of the metal/molecule interface by transient absorption spectroscopy. The overall structure of the sample consists of a mesoporous nanostructured metal oxide film, that acts as a host for the adsorbate-covered metal nanoparticles (see Fig. S1).

The three dimensional nanostructured samples were prepared by wet-grafting of initial Au NPs of 1.7± 0.4 nm in diameter derivatized with mercapto succinic acid (MSA) into the pores of a TiO_2 mesoporous thin film. Before the insertion of gold NPs, the TiO_2 nanocrystalline films exhibit a porosity of 60 % with an average pore size of 20 nm (see Fig. S2).

The capping molecules to stabilize the small gold nanoparticles were chosen in order to be able to form a molecular bridge between TiO_2 and Au nanoparticles. MSA appears as good candidate for this purpose. Aqueous solution of primary 1.7 nm gold NPs were synthesized by $NaBH_4$ reduction of $AuCl_4^-$ in a mixture of water and methanol. The synthesis includes five consecutive washing and centrifugation steps with pure methanol. This sequence ensures the removal of inorganic ions. The solvent excess was evaporated at temperatures below 40°C and a pressure lower than $5 \cdot 10^{-3}$ Torr for 12 h. The core size of the resulting particles exhibited an average diameter of (1.7 ± 0.4) nm.

Carboxylates groups of mercapto succinic acid act as anchors to attach the 1.7 nm Au NPs into the pores of TiO_2 film. Indeed, carboxylate groups are known to bind strongly onto TiO_2 surface via a bidentate binuclear coordination mode.[1]

The final gold NPs used to perform laser spectroscopic measurements were obtained by heat treatment generating sulfate-covered gold nanoparticles of 2.5 to 9.2 nm in diameter. The sizes of the gold NPs have

been revealed by transmission electronic microscopy using a Philips CM20 (see Fig. S3). The sulfate molecules result from the complete oxidation of the molecular bridge (mercapto succinic acid) as revealed by FT-Infrared spectroscopy (see Fig. S4) and X-ray photoemission spectroscopy. Previous studies using similar material for catalysis has also reported the formation of sulfate molecules as a result of heat treatment.[2]

Advantages of transparent mesoporous nanoarchitectures to perform transient absorption study on interfacial phenomena.

Time-resolved optical spectroscopic techniques permit obtaining real-time information on heterogeneous electron transfer reactions. Most of the ultrafast investigations on adsorbates/metal systems have been performed with time resolved two-photon photoemission (a surface sensitive technique) since it is difficult to perform measurements on metal/molecule interfaces due to the very weak signal arising from a monolayer of adsorbates. However, the use of adsorbates-covered metal nanoparticles dispersed in a mesoporous film allows the study of electronic surface phenomena by overcoming this technical problem since the huge surface area of the collection of adsorbates-covered metal NPs permits the enhancement of the signal amplitude. For example, with a 5 μm thick mesoporous film, the signal is increased about 800 times compared to a metal surface covered by a monolayer of adsorbates.[3] This approach has opened avenue to investigate ultrafast charge transfer processes by transient absorption spectroscopy.

Box 2.

Transient absorption spectroscopy of nonequilibrium electrons in noble metal:

Nonequilibrium electrons exhibit complicated dynamics since the optical spectra response in the visible region is dependent on the pump fluence as well as on the probe wavelength. Fig S5 illustrates the different steps of energy redistribution upon the absorption of femtosecond laser pulse by a metal. It should be noted that these steps are not necessary sequential but can overlap in time.

The spectral map of nonequilibrium electrons can be divided in three regions, depending the behaviour and the sign of the signal (see Fig. S6).

Region I: Probe wavelengths shorter than 580 nm: Only negative signals are recorded.

Region II: Probe wavelengths between 580 and 605 nm: Within this region, the sign of the signals are changing. First, the signals are negative, followed by a positive signal.

Region III: Probe wavelengths between 605 and 700 nm: Only positive signals are recorded.

Within region I at the vicinity of *d*-band to Fermi surface transition, the overlap of nonthermal electrons and hot electron gas responses leads to complicated responses at early times, where a negative signal is recorded at any time of process. A fast bleach is formed (not necessary within the instrument response) followed by a bi-exponential recovery (fast component for hot electron cooling followed by a slow component for heat dissipation toward environment). This spectral region has been extensively probed to investigate the external thermalization (hot electron cooling).

Within region II at lower energy than interband transition, the signal exhibits a change of sign, which is expected in view of the transient absorption spectra. A bleach (negative signal), which is formed within the instrument response, reflects the instantaneous creation of nonthermal electrons (as photoexcited). followed by a recovery to give a positive signal, which further decays slowly to the baseline. The change of sign in region II is directly linked to the slow internal thermalization observed with the adsorbate-covered metal nanoparticles. In spectra region II, by probing with shorter wavelengths (closer to interband transition threshold), the signal is more sensitive to thermalized electrons. The absence of fast decay reflects the simultaneous occurrence of electron-electron and electron-phonon interaction:

Within region III, only a positive signal is observed with a rise slower compared to instrumental response. Since this transient absorption is fully linked to the response of hot electron gas (thermal electron distribution), it is possible to follow the formation of the hot electron gas with the rise of the signal in this region. The dynamics of electrons in the energy range of 0.3 to 0.5 eV are monitored in this region. *In summary, It indicates that the lifetime of internal thermalization can be unambiguously extracted from the rise of the signal in region III.*

Section B:

Fitting procedure for the extraction of the internal thermalization lifetimes:

The signals have been fitted, depending on the temporal shapes, with the functions defined below:

$$S(t) = Ae^{-\frac{t}{\tau_1}} + A'e^{-\frac{t}{\tau_1'}} + C \qquad \text{Eq. 1}$$

In this expression, τ_1 and τ_1' represent the two components of the internal thermalization dynamics. The constant C is added to account for the long-lived signal due to the heated lattice. For the transient absorption data obtained at 590 nm, the signals can be fitted with Eq. 1. We note that the signal obtained at this probe wavelength also contains a weak contribution from the electron-phonon interaction (external thermalization). Within spectral region II, as we probe with shorter wavelengths (closer to the d-band to Fermi surface transition), the contribution from external

thermaliaztion becomes more important with respect to the internal thermalization The modulations in the signal obtained at high pump fluences are due to weak damped oscillations superimposed on the exponential decay.

$$S(t) = e^{-\frac{t}{\tau_2}} \cdot \left[1 - \left(A e^{-\frac{t}{\tau_1}} + A' e^{-\frac{t}{\tau_1'}} \right) \right] + C \qquad \text{Eq. 2}$$

In this expression, τ_1 and τ_1' represent the rise time and τ_2 the decay time. At this wavelength, τ_1 and τ_1' reflects the internal thermalization time whereas τ_2 corresponds to the external thermalization (electron-phonon coupling),

$$S(t) = B e^{-\frac{t}{\tau_2}} \cdot \left(1 - e^{-\frac{t}{\tau_1}} \right) + C \qquad \text{Eq. 3}$$

Finally, when the rise time of the signal is composed of two components (τ_1 and τ_1'), the lifetime of internal thermalization τ_{IT} is defined as (with A and A' the amplitude of τ_1 and τ_1', respectively):

$$\tau_{IT} = \frac{A_1 + A_1'}{\left(\frac{A_1}{\tau_1} + \frac{A_1'}{\tau_1'} \right)}$$

In summary,

Fig. 2a: All the signals have been fitted with Eq. 1.

Fig. 2b: All the signals have been fitted with Eq. 2.

Fig. 2c: Signals obtained with photon flux of 125 and 250 nJ/pulse were fitted with Eq. 3 and signals obtained with 305, 450 and 520 nJ/pulse were fitted with Eq. 2.

Fig, 2d: All the signals were fitted with Eq. 3.

References:

(1) Bauer, C.; Boschloo, G.; Mukhtar, E.; Hagfeldt, A.; J. Phys. Chem. B. **2002**; *106*. 12693-12704.
(2) Pietron, J. J.; Stroud, R. M.; Rolison, D. R. *Nano. Lett.* **2002**, *2*, 545.
(3) Tachibana, Y. Thesis Dissertation, Imperial College, London, 1999.

Figure Captions:

Fig. S1. Scanning Electron Micrograph image of three dimensional mesoporous TiO_2 nanostructured film acting as host for the adsorbate-covered metal nanoparticles. The average size of the pores is 20 nm as measured by BET.

Fig. S2. Schematic illustration of the preparation method of the samples.

Fig. S3. Transmission Electron Micrograph images

a. Transmission electron micrograph (TEM) image of mesoporous TiO_2 film.

b. TEM image of 1.7 nm mercapto succinic acid protected Au nanoparticle (before heat treatment)

c. TEM image of 9.2 sulfate-covered Au nanoparticles after heat treatment.

Fig. S4. FT-IR spectrum of sulfate-covered gold metal nanoparticles dispersed into the pores of metal oxide nanostructured films.

Fig. S5. **Schematic diagram of the different steps of energy redistribution in metal NPs upon the absorption of fs laser pulse: Electron-electron scattering, electron-phonon interaction and heat dissipation toward environment.**

Nascent nonthermal electrons created upon the absorption of a femtosecond laser pulse dissipate the excess energy among free electrons via e-e scattering and leads the formation of a hot electron gas with a well defined electronic temperature, the process P_I is called internal thermalization and corresponds to the build-up of a Fermi-Dirac distribution.

The electron-molecular vibration scattering is a process specific to the adsorbates/metal systems and occurs via a bidirectional inelastic electron tunneling into adsorbates.

During the external thermalization (P_{II}), the hot electron gas transfers the energy to the lattice through electron-phonon coupling.

Finally, the last process corresponds to the heat dissipation toward the surrounding medium via phonon-medium coupling (P_{III}).

Fig. S6. Differential transient absorption spectra of 9.2 nm sulfate-covered gold nanoparticles and different spectral regions.

a. Spectra were recorded 200 fs and 5 ps after pumping at 480 nm. The arrows in the bottom show the different spectral regions.

Example of signal recorded in spectral region I, **b**, in spectral region II, **c** and spectral region III, **d.**

Fig. S7. **Correlations between steps of energy redistribution and transient absorption signal shapes in spectral region III.**

At low pump fluence (orange data), a clear separation between P_I, P_{II} and P_{III} can be observed. The lifetime of P_I is given by the rise time of the signal (which occurs within the instrument response), P_{II} by the fast decay ~ 2ps and P_{III} by the slow component (~ 100 ps).

At high pump fluence (black data), P_I is well defined by the rise of the signal. The separation of external thermalization (P_{II}) from heat dissipation (P_{III})is less clear because of the temporal overlap between the two processes.

Fig. S1

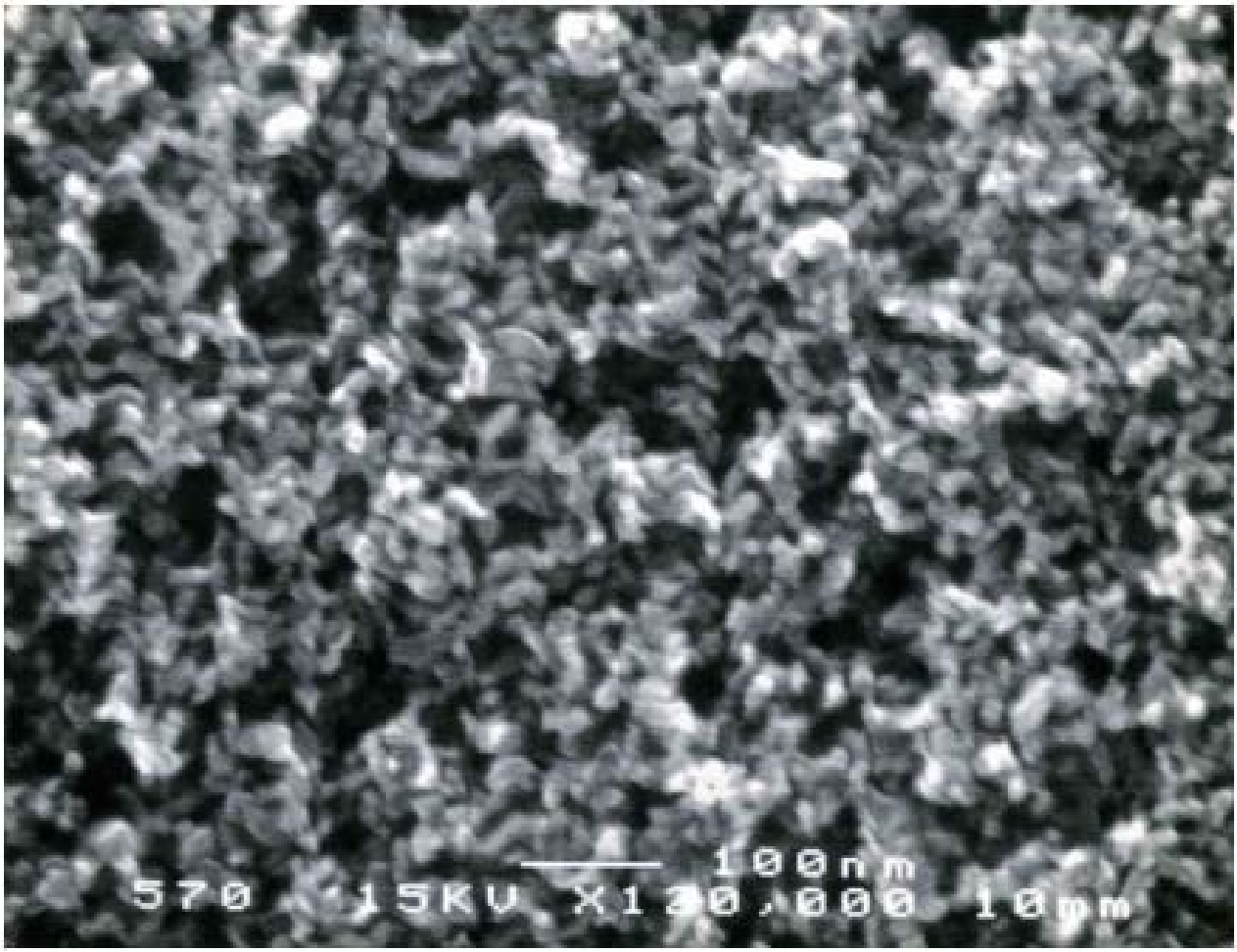

Fig. S2

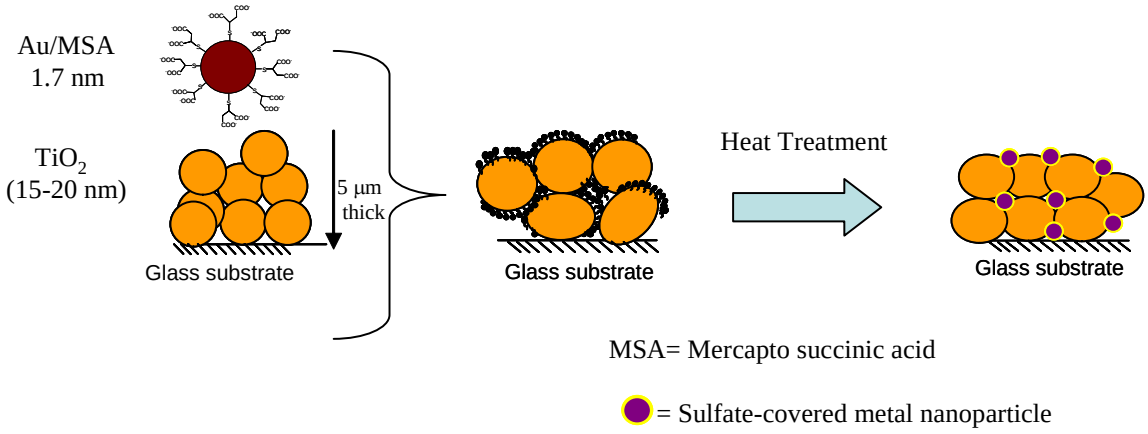
Au/MSA
1.7 nm
TiO2
(15-20 nm)
5 μm
thick
Glass substrate
Glass substrate
Heat Treatment
Glass substrate
MSA= Mercapto succinic acid
= Sulfate-covered metal nanoparticle

Fig. S3

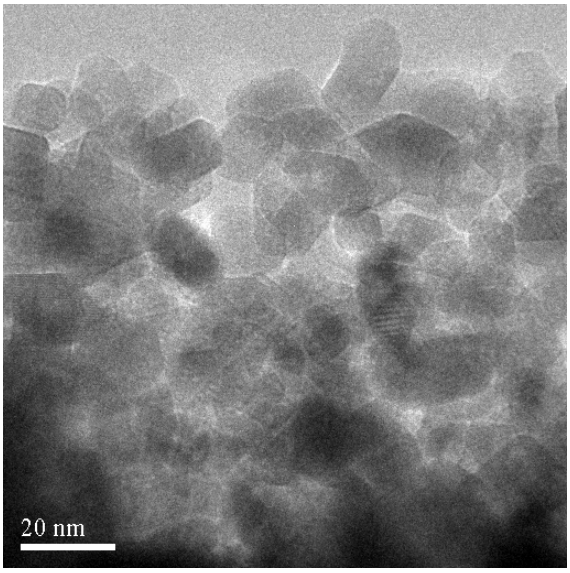

Naked TiO_2

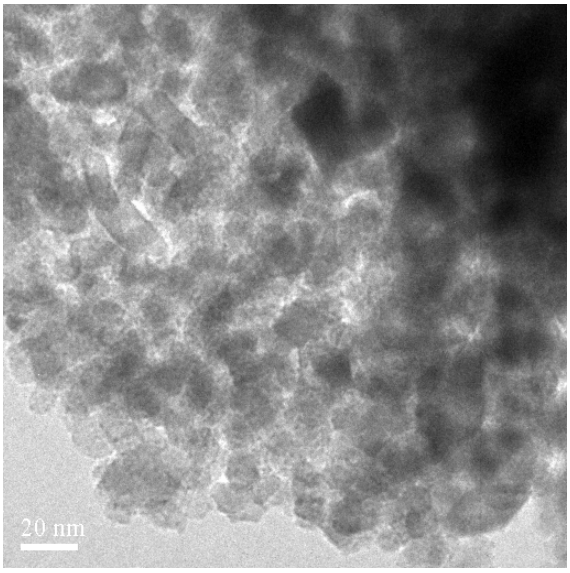

Au/MSA of 1.7 nm inserted into the pores of the TiO_2 film

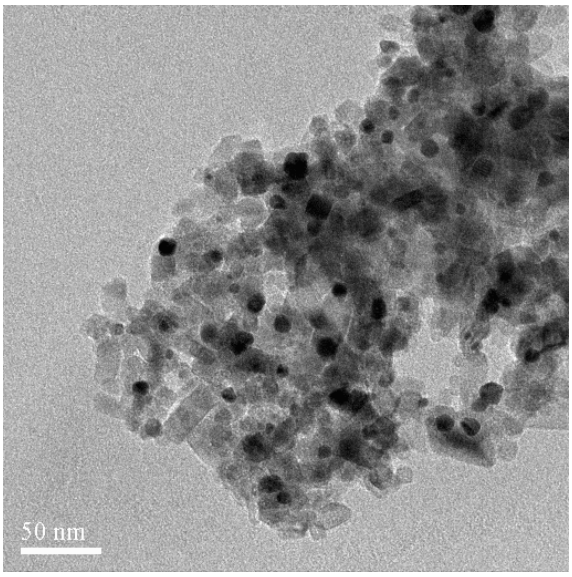

Sulfate-covered gold NPS of 9.2 nm grown into the pores of the TiO_2 film

Fig. S4

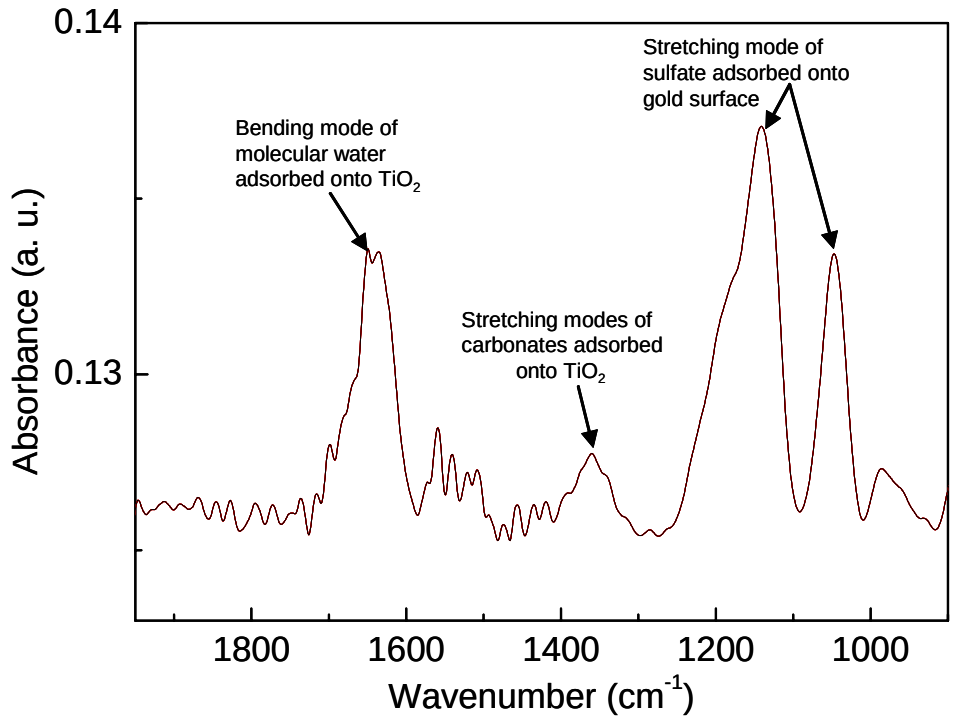
0.14
0.13
Absorbance (a. u.)
Bending mode of molecular water adsorbed onto TiO2
Stretching modes of carbonates adsorbed onto TiO2
Stretching mode of sulfate adsorbed onto gold surface
1800
1600
1400
1200
1000
Wavenumber (cm-1)

Fig. S5

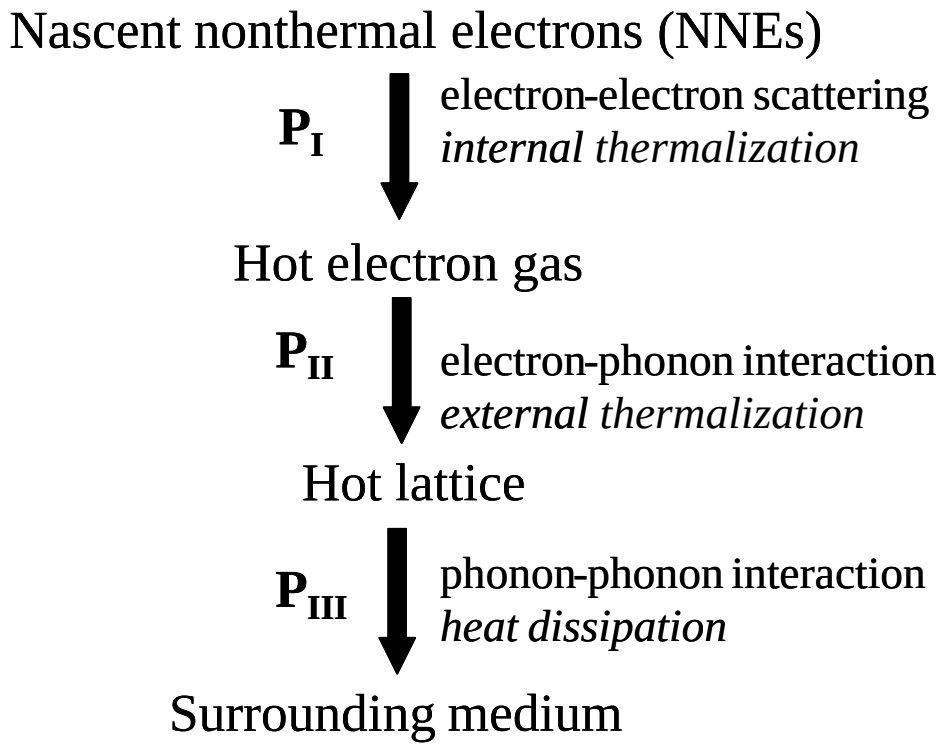
Nascent nonthermal electrons (NNEs)
P_I
electron-electron scattering
internal thermalization
Hot electron gas
P_II
electron-phonon interaction
external thermalization
Hot lattice
P_III
phonon-phonon interaction
heat dissipation
Surrounding medium

Fig. S6

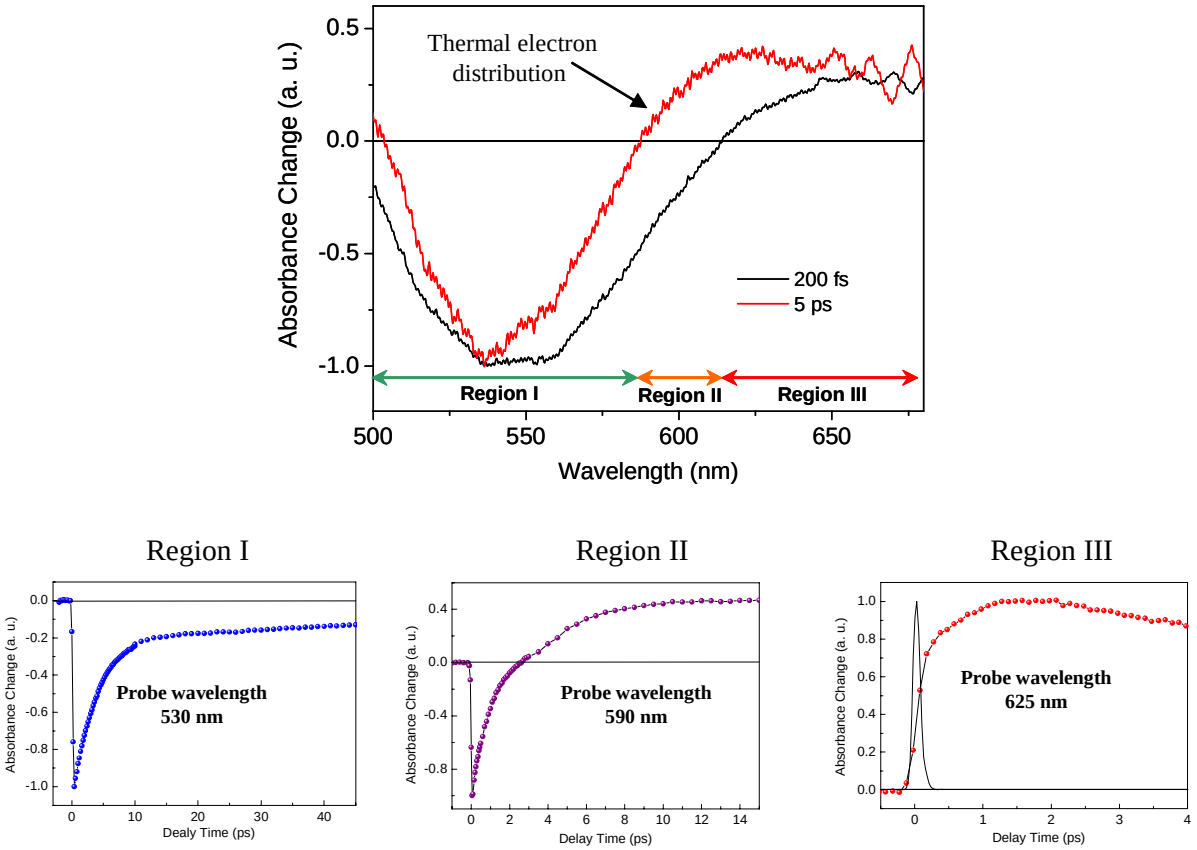
Thermal electron distribution
Absorbance Change (a. u.)
Wavelength (nm)
200 fs
5 ps
Region I
Region II
Region III
Region I
Region II
Region III
Probe wavelength 530 nm
Probe wavelength 590 nm
Probe wavelength 625 nm
Dealy Time (ps)
Delay Time (ps)

Fig. S7

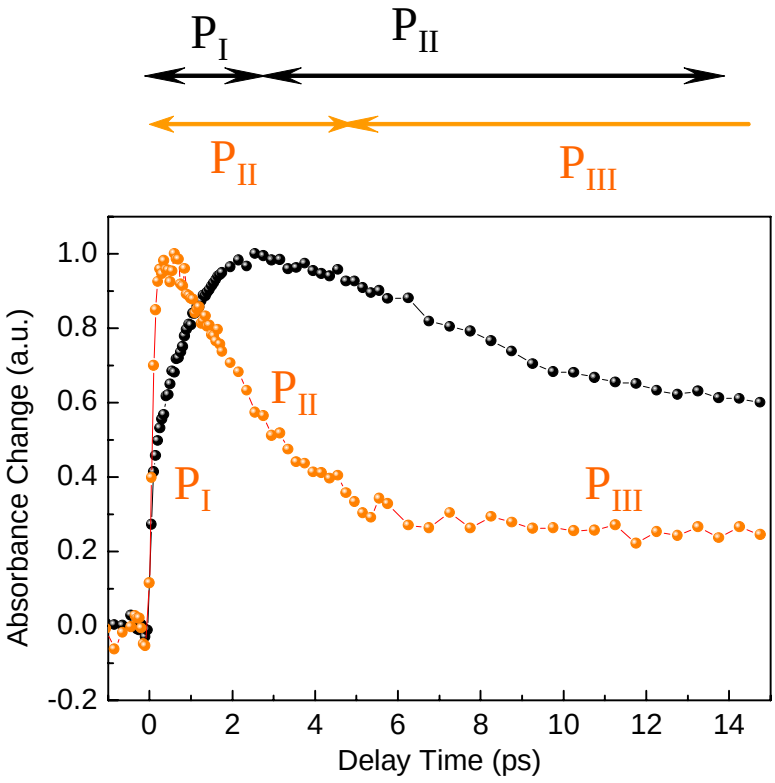
P_I
P_II
P_II
P_III
1.0
0.8
0.6
0.4
0.2
0.0
-0.2
Absorbance Change (a.u.)
P_II
P_I
P_III
0
2
4
6
8
10
12
14
Delay Time (ps)